Articles

The Antibacterial Peptide Pyrrhocoricin Inhibits the ATPase Actions of DnaK and Prevents Chaperone-Assisted Protein Folding†

Goran Kragol,‡ Sandor Lovas,§ Gyorgyi Varadi,‡ Barry A. Condie,‡ Ralf Hoffmann,|| and Laszlo Otvos, Jr.*,‡

The Wistar Institute, 3601 Spruce Street, Philadelphia, Pennsylvania 19104, Biologisch-Medizinisches Forschungszentrum, Heinrich-Heine-Universität, Moorenstrasse 5, 40225 Düsseldorf, Germany, and Department of Biomedical Sciences, School of Medicine, Creighton University, 2500 California Plaza, Omaha, Nebraska 68178

Received November 20, 2000; Revised Manuscript Received January 11, 2001

ABSTRACT: Recently, we documented that the short, proline-rich antibacterial peptides pyrrhocoricin, drosocin, and apidaecin interact with the bacterial heat shock protein DnaK, and peptide binding to DnaK can be correlated with antimicrobial activity. In the current report we studied the mechanism of action of these peptides and their binding sites to *Escherichia coli* DnaK. Biologically active pyrrhocoricin made of L-amino acids diminished the ATPase activity of recombinant DnaK. The inactive D-pyrrhocoricin analogue and the membrane-active antibacterial peptide cecropin A or magainin 2 failed to inhibit the DnaK-mediated phosphate release from adenosine 5′-triphosphate (ATP). The effect of pyrrhocoricin on DnaK's other significant biological function, the refolding of misfolded proteins, was studied by assaying the alkaline phosphatase and β-galactosidase activity of live bacteria. Remarkably, both enzyme activities were reduced upon incubation with L-pyrrhocoricin or drosocin. D-Pyrrhocoricin, magainin 2, or buforin II, an antimicrobial peptide involved in binding to bacterial nucleic acids, had only negligible effect. According to fluorescence polarization and dot blot analysis of synthetic DnaK fragments and labeled pyrrhocoricin analogues, pyrrhocoricin bound with a K_d of 50.8 μM to the hinge region around the C-terminal helices D and E, at the vicinity of amino acids 583 and 615. Pyrrhocoricin binding was not observed to the homologous DnaK fragment of *Staphylococcus aureus*, a pyrrhocoricin nonresponsive strain. In line with the lack of ATPase inhibition, drosocin binding appears to be slightly shifted toward the D helix. Our data suggest that drosocin and pyrrhocoricin binding prevents the frequent opening and closing of the multihelical lid over the peptide-binding pocket of DnaK, permanently closes the cavity, and inhibits chaperone-assisted protein folding. The biochemical results were strongly supported by molecular modeling of DnaK−pyrrhocoricin interactions. Due to the prominent sequence variations of procaryotic and eucaryotic DnaK molecules in the multihelical lid region, our findings pave the road for the design of strain-specific antibacterial peptides and peptidomimetics. Far-fetched applications of the species-specific inhibition of chaperone-assisted protein folding include the control of not only bacteria but also fungi, parasites, insects, and perhaps rodents.

The war between man and bacteria entered a new phase (*1*). With the emergence of antimicrobial-resistant bacterial strains, the currently used drug families start to fail, and a desperate call for a new armory of agents is heard (*2*). Indeed, apart from the discovery of natural antibacterial peptides from plants and animals, there have been few new antibiotics developed in recent years (*2*). In addition, it is now widely accepted that the traditional screening methods, based on direct measurements in living cells of the inhibitory capacities of particular compounds, are unlikely to generate many promising molecules (*3*). One possible alternative strategy is to identify a molecular target at the outset and to design molecules with high affinity and specificity. Ideally, one wants to be able to design antimicrobial compounds specific for a given or just a few bacterial strains or fungi.

Most antimicrobial peptides kill bacteria by inhibiting some bacterial functions but do not have a specific macromolecular target. For example, the cecropins, defensins, and magainins all act on the cell membrane (*4*); buforin II binds nonspecifically to bacterial DNA (*5*). Some other antimicrobial peptides, such as the histatins or NAP-2, are known to act as inhibitors of enzymes produced by the bacteria either by serving as a pseudosubstrate or by tight binding to the active site, eliminating the accessibility of the native substrate (*6*). Perhaps the most promising among the antibacterial peptides with target proteins are the small, proline-rich peptides originally isolated from insects. Apidaecin, drosocin,

† This work was supported by NIH Grant GM 45011 and NSF Grant EPS-9720643. Additional funds were provided by the Principal Investigator.

* To whom correspondence should be addressed. Tel: 215-898-3772. Fax: 215-898-5821. E-mail: Otvos@wistar.upenn.edu.

‡ The Wistar Institute.

§ Creighton University.

|| Heinrich-Heine-Universität.

10.1021/bi002656a CCC: $20.00
Published on Web 02/10/2001

and pyrrhocoricin were suggested to kill bacteria by acting stereospecifically on a bacterial protein (*7*−*9*). The proposed mechanism by which apidaecin kills bacteria involves an initial, nonspecific encounter of peptide with an outer membrane component, followed by invasion of the periplasmic space and by a specific and essentially irreversible engagement with a receptor/docking molecule that may be inner membrane-bound or otherwise associated, most likely a component of a permease-type transporter system. In the final step, the peptide is translocated into the interior of the cell where it meets its ultimate target, perhaps one or more components of the protein synthesis machinery (*10*). When identifying the biopolymers involved in this cascade, we observed that pyrrhocoricin, drosocin, and apidaecin bind to the bacterial lipopolysaccharide (LPS)[1] and the 70 kDa heat shock protein DnaK in a specific manner and the 60 kDa bacterial chaperonine GroEL in a nonspecific manner (*11*). The antibacterial actions and DnaK binding can be positively correlated because an inactive pyrrhocoricin analogue, made of all D-amino acids, does not interact with DnaK (*11*).

Although we speculated that DnaK is the ultimate target and not only a temporary player in the cell entry and transport processes (*11*), experimental proof for inhibiting DnaK actions has not yet been provided. In the current report we investigated how pyrrhocoricin and drosocin affect DnaK's two major functions, the ATPase activity and refolding of misfolded proteins. The modification of the ATPase activity was studied with a commercially available recombinant DnaK preparation and direct measurements of phosphate release from ATP. The protein folding ability was assessed by measuring the enzymatic activity of live bacteria upon incubation with antibacterial peptides.

It is known that both termini of pyrrhocoricin are required to exhibit the antibacterial activity (*9*). These two ends need to be covalently connected as a mixture of the two halves fail to kill bacteria (*12*). Competition fluorescence polarization suggested two independent pyrrhocoricin binding sites on DnaK (*11*). On the basis of a comparison of the DnaK sequences of pyrrhocoricin-responsive and pyrrhocoricin-nonresponsive bacteria, we speculated that at least one binding site on DnaK is probably located between the conventional peptide-binding pocket and the extreme C-terminus of the protein. In the current report we identified the hinge region between helices D and E as the site where the N-terminus of pyrrhocoricin binds to DnaK. In addition to binding to the multihelical lid, pyrrhocoricin may also interact with the conventional peptide-binding pocket. Hereby, we propose a mechanism by which the proline-rich antibacterial peptides kill bacteria by preventing the frequent movements of the multihelical lid over the peptide binding cavity. By permanently closing the multihelical lid over the peptide-binding pocket, the peptides inhibit chaperone-assisted protein folding. In addition, we show that the other major biological function of DnaK, the ATPase activity, is also specifically inhibited by pyrrhocoricin.

MATERIALS AND METHODS

Synthetic Peptides. The following DnaK fragments were synthesized: (a) *Escherichia coli* DnaK 397−439, the conventional peptide binding pocket; (b) *E. coli* DnaK 513−551, the hinge region between C-terminal helices A and B, containing the entire B-helix, which is located just above the peptide binding pocket; (c) *E. coli* DnaK 583−615, the hinge region between C-terminal helices D and E, located also in the multihelical lid, slightly further away from the peptide binding pocket; (d) N-terminally truncated forms of the *E. coli* D−E helix peptide, such as 588−615, 590−615, and an N-terminally blocked 591−615 analogue; (e) *Staphylococcus aureus* DnaK 554−585, the structural analogue of the *E. coli* 583−615 peptide; and (f) *E. coli* DnaK 596−637, the flexible region between the multihelical lid and the extreme C-terminus.

The sequences of the native antibacterial peptides discussed in this paper are as follows: drosocin, GKPRPYSPRPT-SHPRPIRV; pyrrhocoricin, VDKGSYLPRPTPPRPIYNRN; apidaecin 1a, GNNRPVYIPGPRPPHPRI. Native drosocin and pyrrhocoricin are glycosylated on the underlined threonines, but as the attached sugar moieties are not required for the antibacterial activity, the peptides used in this study did not contain carbohydrate side chains.

Other peptides included the negative control conantokin G, an *N*-methyl-D-aspartate (NMDA) receptor antagonist (*13*); pyrrhocoricin made of all D-amino acids; magainin 2, an antibacterial peptide that kills bacteria by disintegrating the membrane (*14*); cecropin A, another membrane-active antimicrobial peptide (*15*); buforin II, an antibacterial peptide that binds to bacterial DNA (*5*); the N-terminal 1−9 and C-terminal 10−20 halves of pyrrhocoricin; biotin-labeled L- and D-pyrrhocoricin (*12*); fluorescein-labeled pyrrhocoricin, drosocin, and apidaecin (*11*); the pyrrhocoricin two halves also labeled with fluorescein; fluorescein- and biotin-labeled β-tubulin fragment 434−445 serving as negative controls (*16*, *17*); and another negative control fluorescein-labeled peptide with the sequence NTDGSTDYGILQINSR.

Pyrrhocoricin, drosocin, apidaecin 1a, their fragments and labeled variants, conantokin G, and the *E. coli* and *S. aureus* DnaK fragments as well as the negative control labeled peptides were made by standard solid-phase methods (*18*). The peptides were purified by reversed-phase high-performance liquid chromatography, and their integrity was verified by laser desorption and electrospray ionization mass spectrometry. The actual peptide content of the lyophilized samples was chromatographically determined (*19*). Buforin II was purchased from Sigma (St. Louis, MO); cecropin A and magainin 2 were purchased from Bachem (King of Prussia, PA).

ATPase Activity Assay. Recombinant DnaK protein was purchased from StressGen (Victoria, Canada). ATPase activity was assayed by a spectrophotometric method (*20*) using 2-amino-6-mercapto-7-methylpurine ribonucleoside (MESG)/purine nucleoside phosphorylase reaction to detect the released inorganic phosphate (EnzChek kit from Molecular Probes, Eugene, OR). Assays were performed in 500 μL tubes in a total volume of 125 μL containing 20 mM tris-

[1] Abbreviations: ADP, adenosine 5′-diphosphate; ATP, adenosine 5′-triphosphate; BSA, bovine serum albumin; EDTA, ethylenediaminetetraacetic acid; HRP, horseradish peroxidase; LPS, lipopolysaccharide; MD, molecular dynamics; MESG, 2-amino-6-mercapto-7-methylpurine ribonucleoside; NMDA, *N*-methyl-D-aspartate receptor; NMR, nuclear magnetic resonance spectroscopy; PBS, phosphate-buffered saline; PBST, phosphate-buffered saline−Tween 20 buffer; Tris, tris(hydroxymethyl)aminoethane; UV, ultraviolet.

(hydroxymethyl)aminoethane hydrochloride (Tris-HCl), pH 7.6, 1 mM $MgCl_2$, 300 mM ATP (except in assaying the baseline), 5 μg of DnaK, and 50 molar equiv of the particular peptide, MESG and the purine nucleoside phosphorylase recommended by the manufacturer. After incubation at 22 °C for 30 min, 100 μL of the reaction mixture was transferred to a quartz cuvette, and the ultraviolet (UV) absorbance at 360 nm was measured.

Treatment of the Live E. coli Culture. A 5 mL culture was shaken at 37 °C for 5−6 h, then 300 μL was added to 30 mL of Luria−Bertani rich nutrient medium, and the bacterial culture was shaken at 37 °C overnight. Sixteen microliters of a 1 μg/μL peptide solution was added to 500 μL of the overnight culture, and the mixture was incubated at 30 °C for 1−6 h. After the incubation period expired, the cells were harvested with a 2 min sonication on a probe sonicator and were centrifuged for 20 min at 3000*g*. The supernatant was used for the ensuing β-galactosidase and alkaline phosphatase assays.

Enzymatic Assays. (1) β-Galactosidase: 50 μL of cell lysate was added into the wells of a 96-well plate. One hundred ten microliters of a 100 mM phosphate-buffered saline (PBS), pH 7.5, containing 1 mM $MgSO_4$/β-mercaptoethanol mixture (95:5 v/v) was added to the wells, and the plate was covered and incubated at 37 °C for 5 min. Fifty microliters of a 4 mg/mL *o*-nitrophenyl β-D-galactopyranoside substrate solution was added to each well, and the plate was incubated at 37 °C until the well contents turned bright yellow. The reaction was terminated by adding 90 μL of 1 M Na_2CO_3 solution, and the plate was scanned by a microtiter dish reader set at 405 nm. (2) Alkaline phosphatase: 50 μL of cell lysate was added into the wells of a 96-well plate. One hundred ten microliters of a 1.5 M 2-amino-2-methyl-1-propanol buffer, pH 10.3, was added to the wells, and the plate was covered and incubated at 37 °C for 5 min. Fifty microliters of a 4.9 mg/mL *p*-nitrophenyl disodium phosphate substrate solution was added to each well, and the plate was incubated at 37 °C until the well contents turned bright yellow. The reaction was terminated by addition of 90 μL of a 1 M H_3PO_4 solution, and the plate was scanned by a microtiter dish reader set at 405 nm.

Dot Blot Assay. The DnaK fragments were dissolved in electroblot transfer buffer (25 mM Tris and 192 M glycine buffer containing 20% methanol) and were applied to a nitrocellulose membrane. The membrane was blocked with 5% milk in a PBS−0.5% Tween 20 buffer (PBST) for 3 h at room temperature and was incubated with 10 mL of 10 μg/mL biotin-labeled peptides dissolved in PBST containing 1% bovine serum albumin (BSA) for 1 h. After incubation, the membrane was extensively washed with PBST. Streptavidin conjugated to horseradish peroxidase (HRP) (Gibco-BRL) dissolved in 1% BSA−PBST was added to the membrane and was incubated at room temperature for 45 min. After extensive washing with PBST, the membrane was treated with chemiluminescence luminol oxidizer (NEN) for 1 min. The created chemiluminescence was exposed to a X-Omat blue XB-1 film (Kodak) for 10 s, and the film was developed. A control strip was stained with amido black 10B to verify the presence of all DnaK fragments on the nitrocellulose sheet.

Fluorescence Polarization. Binding of the synthetic DnaK fragments to their fluorescein-labeled counterparts in solution was assessed by fluorescence polarization (*21*). For these experiments, the unlabeled peptides were serially diluted in PBS (pH 7.4) or 0.1 M Tris-HCl (pH 8.0) containing 0.1 M ethylenediaminetetraacetic acid (EDTA) in 50 μL final volume in 6 × 50 mm disposable glass borosilicate tubes. The fluoresceinated peptides were added to each tube in a 50 μL aliquot to a final concentration of 1 nM, and tubes were incubated at 37 °C for 5 min. The extent of fluorescence anisotropy was measured on a Beacon 2000 fluorescence polarization instrument (PanVera, Madison, WI) and calculated as millipolarization values. The filters used were 485 nm excitation and 535 nm emission with 3 nm bandwidth. Nonlinear curve fitting was done by using a dose−response logistical transition [$y = a_0 + a_1/(1 + x/a_2)^{a_3}$] and the Levenberg−Marquardt algorithm within the SlideWrite software package. The provided K_d value (a_2 coefficient) was calculated by the program.

Molecular Modeling. To have a well-equilibrated structure for docking, the initial coordinate of pyrrhocoricin which was obtained from nuclear magnetic resonance (NMR) analyses (*12*) was subjected to molecular dynamics (MD). Structures of the peptide were simulated in two 10 ns constant pressure and constant temperature MD in the presence of 5769 SPC/E water using the GROMACS 2.0 package (*22*). Secondary structures of pyrrhocoricin in trajectories were determined by the DSSP method (*23*). The X-ray coordinate of *E. coli*, PDB ID 1DKX (*24*), was obtained from the Brookhaven Protein Data Bank (*25*). The missing side chain atoms were reconstructed, and all the missing H atoms were added with the SYBYL molecular modeling package. Since the C-terminal tail is missing from the X-ray structure, the protein was elongated with nine residues in order to have the compatibility with the fluorescence polarization experiments. The structure of the added sequence was set to α-helical and was energy minimized with the Tripos force field using the Kollman–all charges, and then the structure of the whole protein was energy minimized with the same parameters as above. The structure of pyrrhocoricin was docked into DnaK using the FlexiDock module of SYBYL. The structure of DnaK was fixed in space, and side chains of residues 397−439 (peptide-binding pocket) and residues 587−615 (helices D and E) were flexible. All bonds, except the peptide bond, were set to be flexible in the structure of pyrrhocoricin. Genetic algorithm search was performed using 0.5 Å grid spacing, 60 000 energy evaluation, and saving the best 40 structures in a database.

RESULTS

Inhibition of ATPase Activity. The protein folding activity of the 70 kDa heat shock protein family is driven by their ATPase activity that regulates cycles of polypeptide binding and release (*26*). Although the region responsible for ATPase actions has been identified at the amino-terminal half of the protein (*27*), the ATPase activity is allosterically modulated by the C-terminal domain of human Hsp70 and its analogue Hsc70 (*28*, *29*). We wanted to see whether the proline-rich antibacterial peptides that we predicted bind to DnaK between the peptide binding pocket and the C-terminus would interfere with ATPase activity. For these experiments we used a recently developed continuous colorimetric assay (*20*). Recombinant DnaK had a small but measurable ATPase

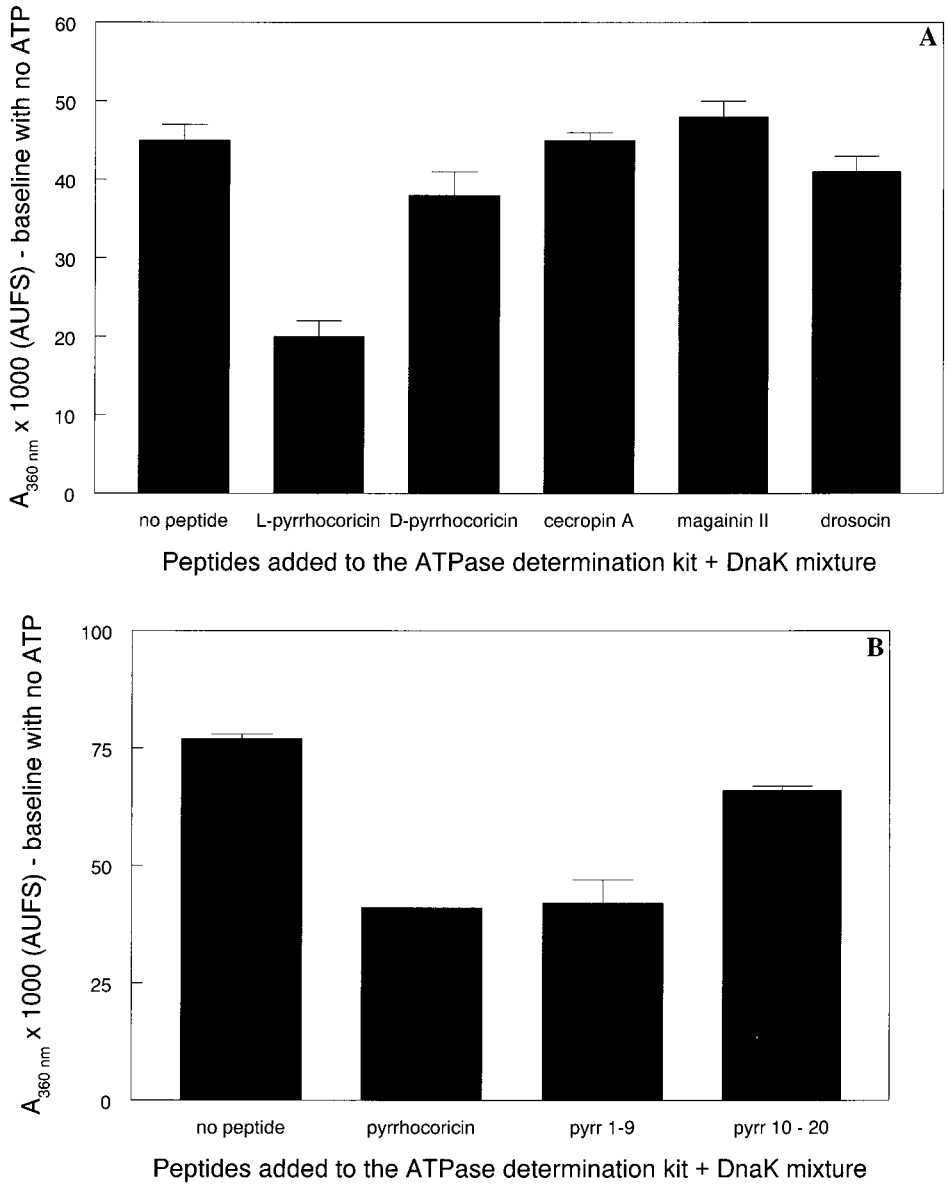

FIGURE 1: Inhibition of ATPase activity of recombinant *E. coli* DnaK by synthetic antibacterial peptides (panel A) and pyrrhocoricin fragments (panel B). Five micrograms of DnaK and 50 molar equiv of peptides were added to the EnzChek ATPase determination kit in duplicates. The assay was run in a miniaturized form to increase the concentration and therefore the enzymatic activity of DnaK. In a larger, standard format the ATPase activity of DnaK without peptide addition was 6 pmol μg^{-1} min^{-1}, in line with the published data of 4 pmol μg^{-1} min^{-1} (*35*).

activity (Figure 1, panel A). The assay was repeated four times with different batches of DnaK and freshly made reagent solutions. During these conditions, the increase of the UV absorbance at 360 nm upon addition of ATP varied from 0.038 to 0.077 AUFS, with a mean value of 0.060 AUFS, reflecting some differences in the quality of the various DnaK preparations. When the biologically active L-pyrrhocoricin was added to the assay mixture, the activity dropped to less than half of the original value (Figure 1, panel A). In contrast, the inactive D-analogue of pyrrhocoricin had negligible effect. These assays were repeated twice and yielded the same reduction in the level of ATPase activity with the actual numbers dependent upon the original enzymatic activity of the different DnaK batches (compare with Figure 1, panel B). Cecropin A and magainin 2, two antimicrobial peptides that kill bacteria by disintegrating the membrane, did not influence the ATPase activity of DnaK, as expected. Interestingly, drosocin, another proline-rich antibacterial peptide, a close relative of pyrrhocoricin, remained without affecting the ATPase activity (Figure 1, panel A). This suggested that pyrrhocoricin and drosocin did not share a common binding site to *E. coli* DnaK. Pyrrhocoricin did not influence the ATPase activity of recombinant Hsp70, the human equivalent of DnaK (0.058 vs 0.063 AUFS).

In the next step we tried to identify the fragment of pyrrhocoricin that is responsible for the inhibition of the ATPase activity. From our earlier studies we know that both termini of pyrrhocoricin are needed to kill bacteria, but the isolated halves alone, or their equimolar mixture, are completely inactive (*12*). When tested for the inhibition of the ATPase activity of recombinant DnaK, the amino-terminal 1−9 fragment of pyrrhocoricin was as effective as full-size pyrrhocoricin itself (Figure 1, panel B). The C-terminal 10−20 fragment also had some minor activity but not as significant as the N-terminal half. Apparently, the

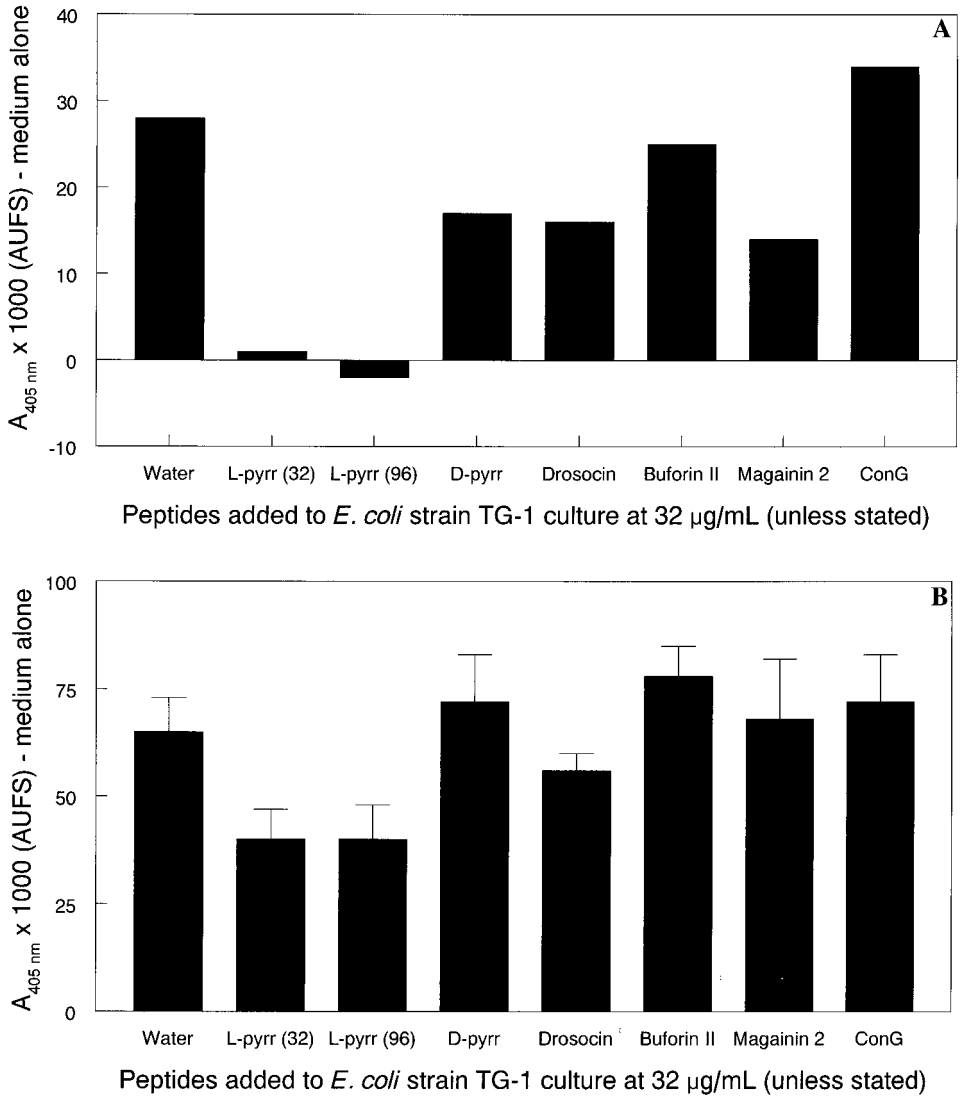

FIGURE 2: Inhibition of β-galactosidase (panel A) and alkaline phosphatase (panel B) activities of live *E. coli* TG-1 cells by synthetic antibacterial peptides. The assays were run as described in the Materials and Methods section. The peptides were added to the *E. coli* cultures at a concentration of 32 μg/mL (except L-pyrrhocoricin was added at either 32 or 96 μg/mL as marked in the figures), which represents a value above the minimal inhibitory concentration of the active peptides, and is regarded as a conventional concentration for a series of standard antibacterial assays (*36*). In this particular assay, the activities of either enzymes (without peptide addition) correspond to approximately 800 pmol well^{-1} min^{-1}. These experiments were repeated two to three times with bacteria growing in different rates as reflected by the increase of the enzymatic activity between 1 and 6 h. The figure shows efficiently growing bacteria plated to duplicate (alkaline phosphatase) or single (β-galactosidase) wells.

amino terminus is a strong binder to the allosteric ATPase site, but the C-terminal half also has some residues capable of binding to this DnaK domain.

Inhibition of Protein Folding As Assayed by Enzyme Activity of Live E. coli Cultures. Pyrrhocoricin strongly inhibited the β-galactosidase activity of an *E. coli* strain TG-1 culture in a peptide concentration-dependent manner (Figure 2, panel A). The inhibitory activity could be detected as early as 1 h after introduction of the peptide. While it was not significantly inhibitory after 1 h during this particular assay, drosocin became detrimental to the β-galactosidase activity after 6 h. When the results of three independent assays were compared, drosocin inhibited the β-galactosidase activity in the entire 1−6 h examination period (Table 1). None of the control peptides, including the all-D analogue of pyrrhocoricin, the membrane-active peptide magainin 2, the DNA-binding antibacterial peptide buforin II, or the irrelevant peptide conantokin G had any β-galactosidase inhibitory effect on live *E. coli* cells (Figure 2, panel A, and Table 1). On the basis of these results, pyrrhocoricin and drosocin inhibited chaperone-assisted protein folding. Both pyrrhocoricin and drosocin had a less dramatic effect on the alkaline phosphatase activity of the bacterial culture (Figure 2, panel B, and Table 1). Nevertheless, the decreased enzymatic activity upon incubation with L-pyrrhocoricin and drosocin, compared with D-pyrrhocoricin, buforin II, magainin 2, or conantokin G, is evident from Figure 2, panel B. These tendencies were more visible when the experiment was repeated with less efficiently growing bacteria, although in this case the reading values were significantly lower and the experimental error became higher. Table 1 summarizes three independent assays for β-galactosidase and four assays for alkaline phosphatase inhibition. Despite the sometimes observed high error rate, the table demonstrates well that only pyrrhocoricin and drosocin inhibit the activity of these enzymes in live *E. coli* cells.

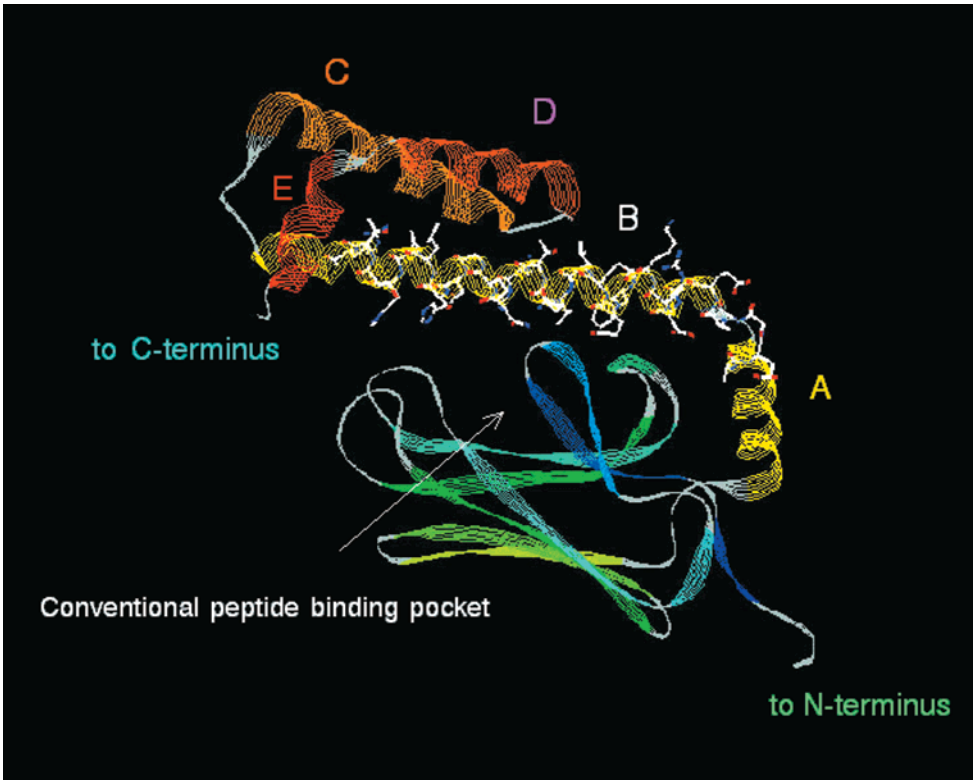

FIGURE 3: Three-dimensional structure of *E. coli* DnaK from the peptide-binding pocket to the C-terminal end of helix E, as represented by Zhu et al. (*24*). The letters indicate the individual helices of the multihelical lid.

Table 1: Inhibition of β-Galactosidase and Alkaline Phosphatase Activities of Live *E. coli* Cells[a]

	inhibition of enzymatic activity after 1 h (%)	
peptide	β-galactosidase	alkaline phosphatase
L-pyrrhocoricin	153 ± 57	32 ± 16
D-pyrrhocoricin	−4 ± 43	−6 ± 21
drosocin	98 ± 68	35 ± 27
buforin II	−5 ± 33	−6 ± 34
magainin 2	−50 ± 55	−23 ± 38
conantokin G	−10 ± 10	−3 ± 23

[a] This table shows the results of three independent assays for β-galactosidase and four for alkaline phosphatase, run over a 3 week period. The high error value is originated from the differences in the actual stage and rate of bacterial growth in the assay wells. Apparently, the assay conditions need to be perfected and standardized. Nevertheless, for the sake of this report, the table documents well that from all antibacterial peptides tested only L-pyrrhocoricin and drosocin were inhibitory for the enzymatic activity of the bacterial cells. All peptides were applied at a final concentration of 32 μg/mL. The percentages were calculated on the basis of the UV absorbance differences between the wells containing peptides relative to the wells containing distilled water and medium without cells. The above 100% values indicate UV absorbance below that for wells containing medium only; the negative values indicate UV absorbance above that for wells containing cells and distilled water.

Identification of the Pyrrhocoricin-Binding Site on E. coli DnaK. In the earlier report we speculated that pyrrhocoricin binds to DnaK both inside and outside the conventional peptide binding pocket, and the most probable outside binding site is located between the peptide binding cavity and the extreme C-terminus (*11*). The allosteric inhibition of the ATPase activity, as presented above, supported this idea. This, together with the inhibition of the enzymatic activity of live bacteria, and therefore general inhibition of protein folding, suggested that the peptide bound somewhere in the region of the multihelical lid assembly. The structure of the C-terminal domain of DnaK, as derived from the X-ray structure, is shown in Figure 3 (*24*). To identify the actual pyrrhocoricin-binding site(s), we synthesized four fragments of the protein. These fragments corresponded to the peptide-binding cavity, the flexible C-terminus, and two regions that included hinges between helices A and B as well as helices D and E. These C-terminal peptides were made because, on the basis of the biochemical data, we hypothesized that pyrrhocoricin prevents protein folding by binding to one of these DnaK fragments and permanently closes the lid over the peptide-binding pocket. Although an intrahelix hinge was also reported to operate in helix B (*30*), major movements of the multihelical lid likely involve the interhelix flexible domains. First, we used dot blot to study the binding of biotin-labeled pyrrhocoricin to the DnaK fragments. We applied 1 and 5 μg test peptides to the nitrocellulose paper. As control peptides, we used biotin-labeled versions of the inactive D-pyrrhocoricin analogue and the unrelated peptide tubulin, just as in the earlier study dealing with the full-size protein (*11*). Figure 4 shows the results of the assay. The top row represents the blot developed with the effective antibacterial peptide L-pyrrhocoricin, the middle row represents the blot developed with the inactive D-pyrrhocoricin analogue, and the bottom row was developed with tubulin. Earlier, a number of unspecific bands were detected on the Western blot when the interaction between biotin-labeled peptides and the full-size DnaK protein had been studied (*11*). The nonspecific binding was related to interaction with the peptide-binding pocket, as this DnaK fragment similarly bound all three (L-pyrrhocoricin, D-pyrrhocoricin, tubulin) peptides (Figure 4). Some unspecific binding was also observed to the C-terminal flexible domain. Remarkably, at

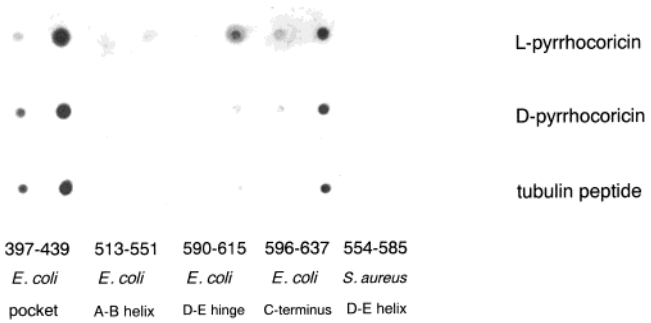

FIGURE 4: Dot blot analysis of binding of DnaK fragments to biotin-labeled L-pyrrhocoricin (top row), biotin-labeled D-pyrrhocoricin (middle row), and biotin-labeled tubulin 434−445 (bottom row). Each peptide was applied to the nitrocellulose in 1 and 5 μg amounts (left to right).

5 μg the bioactive L-pyrrhocoricin bound to another DnaK fragment, the hinge region between helices D and E, at residues 590−615. This binding site appeared to be specific, as only very weak staining was observed to biotin-labeled D-pyrrhocoricin or tubulin (Figure 4). The fourth *E. coli* DnaK fragment, corresponding to the A−B helix region, was not stained. The selectivity of pyrrhocoricin to some bacterial strains could be verified by the lack of binding to the *E. coli* 583−615 analogue *S. aureus* 554−585 fragment (Figure 4). Pyrrhocoricin and most of its designed analogues are inactive against *S. aureus* in vitro (*11*).

The binding of the DnaK fragments to pyrrhocoricin was also studied in solution by fluorescence polarization. A preliminary assay was run in PBS, in conditions and with controls identical to those we used when pyrrhocoricin binding of the full-size DnaK protein was studied (*11*). Due to the low solubility of the peptides, especially corresponding to the *E. coli* DnaK D−E helix 583−615 fragment, this peptide was replaced with a side product of the synthesis. An N-terminally blocked analogue of the 591−615 fragment exhibited somewhat increased solubility in PBS. The fluorescein-labeled pyrrhocoricin peptide bound strongly to the blocked *E. coli* DnaK fragment 591−615 and weakly to fragment 397−439, representing the conventional peptide binding pocket, verifying the results of the dot blot assay. No interaction above the level of the negative control conantokin G peptide was observed for the other two *E. coli* fragments, representing the A−B helix or the extreme C-terminus, or the D−E helix fragment of *S. aureus* DnaK. Fluorescein-labeled drosocin failed to bind to the blocked 591−615 DnaK fragment. As a reverse control we used the D−E helix hinge peptide against the fluorescein-labeled tubulin fragment. Again, no binding was detected. Nevertheless, due to the low solubility of the peptides, these data have to be treated with caution and are presented here only in qualitative terms.

The assay was repeated in Tris-HCl at pH 8.0, where the DnaK fragments exhibited increased solubility. DnaK fragments showing nonspecific binding on the dot blot were not studied. The negative control fluorescein-labeled tubulin peptide was replaced with another labeled peptide, which is not so heavily negatively charged, and potentially less cross-reactive. In Tris-HCl, fluorescein-labeled pyrrhocoricin did not bind to the *E. coli* A−B helix fragment or the *S. aureus* D−E helix fragment over the labeled pyrrhocoricin background, which is indicated by the horizontal lines above the bars (Figure 5, panel A). Drosocin and apidaecin also failed to bind to the *S. aureus* D−E helix. In contrast, a concentration-dependent binding of pyrrhocoricin was observed to the *E. coli* D−E helix hinge region representing amino acids 583−615. This binding appears to be specific as the negative control fluorescein-labeled NTDGSTDYGILQINSR peptide failed to bind to the same *E. coli* D−E helix (Figure 5, panel A). At a high concentration (128 μM) some binding to fluorescein-labeled drosocin and apidaecin was also observed. To quantitatively characterize the pyrrhocoricin−D−E helix interaction, the complete binding curves were measured for *E. coli* DnaK fragments 583−615 and 588−615. The longer D−E helix peptide bound to the labeled pyrrhocoricin with a K_d of 50.8 μM (Figure 5, panel B). The shorter peptide bound with a somewhat decreased efficacy, exhibiting a K_d of 93 μM. This reduction in the binding affinity reflects either the decreased length of the second DnaK fragment or the inherent inaccuracy of the fluorescence polarization measurements. Drosocin also bound to the 588−615 fragment but considerably weaker than pyrrhocoricin. This, together with the lack of drosocin binding to the blocked 591−615 fragment, indicated that while pyrrhocoricin bound to the D−E helix region at the hinge and the E helix area, drosocin binding was somewhat shifted back to the N-terminal direction between the D helix and the hinge. This explains the differences in the ATPase activity inhibiting capacities between pyrrhocoricin and drosocin. When the DnaK binding of the fluorescein-labeled pyrrhocoricin halves were studied, both the 1−9 and the 10−20 fragments strongly bound to the *E. coli* DnaK 588−615 peptide with a 30 millipolarization unit increase going from 32 to 160 μM, indicating that the binding to the DnaK fragment cannot be located only to the N-terminal, ATPase activity reducing segment. Additional experiments to characterize the pyrrhocoricin−DnaK D−E helix interaction by isothermal titration calorimetry and surface plasmon resonance are currently underway, as is the identification of possible independent functions of this DnaK helix domain to establish the optimal conditions for later competitive binding studies.

Molecular Modeling. Two, independently initiated, 10 ns simulations were performed to sample sufficiently the available conformational space for pyrrhocoricin. During both of the MD simulations, the total energy, temperature, and density of the pyrrhocoricin peptide−solvent system came to equilibrium within the first 100 ps, which time was excluded from the conformation analyses. In both simulations the following secondary structures were extensively sampled: β-bridge conformations for residues 2 and 6; β-turn conformations for residues 3−5 and residues 15 and 16. Overall, these data were in good agreement with the previous NMR measurement (*12*). Therefore, as characteristic structure it was selected for flexible docking.

Two initial configurations were set up manually. Either the C-terminal part of pyrrhocoricin was placed into the peptide-binding pocket in such a way that the N-terminal domain of the peptide was close to the D helix region of the protein (docking 1) or the structure of pyrrhocoricin was aligned in antiparallel direction with the D−E helix region of *E. coli* DnaK (docking 2). During docking 1, pyrrhocoricin moved out from the peptide-binding pocket and became located in the area between the multihelical lid and the pocket

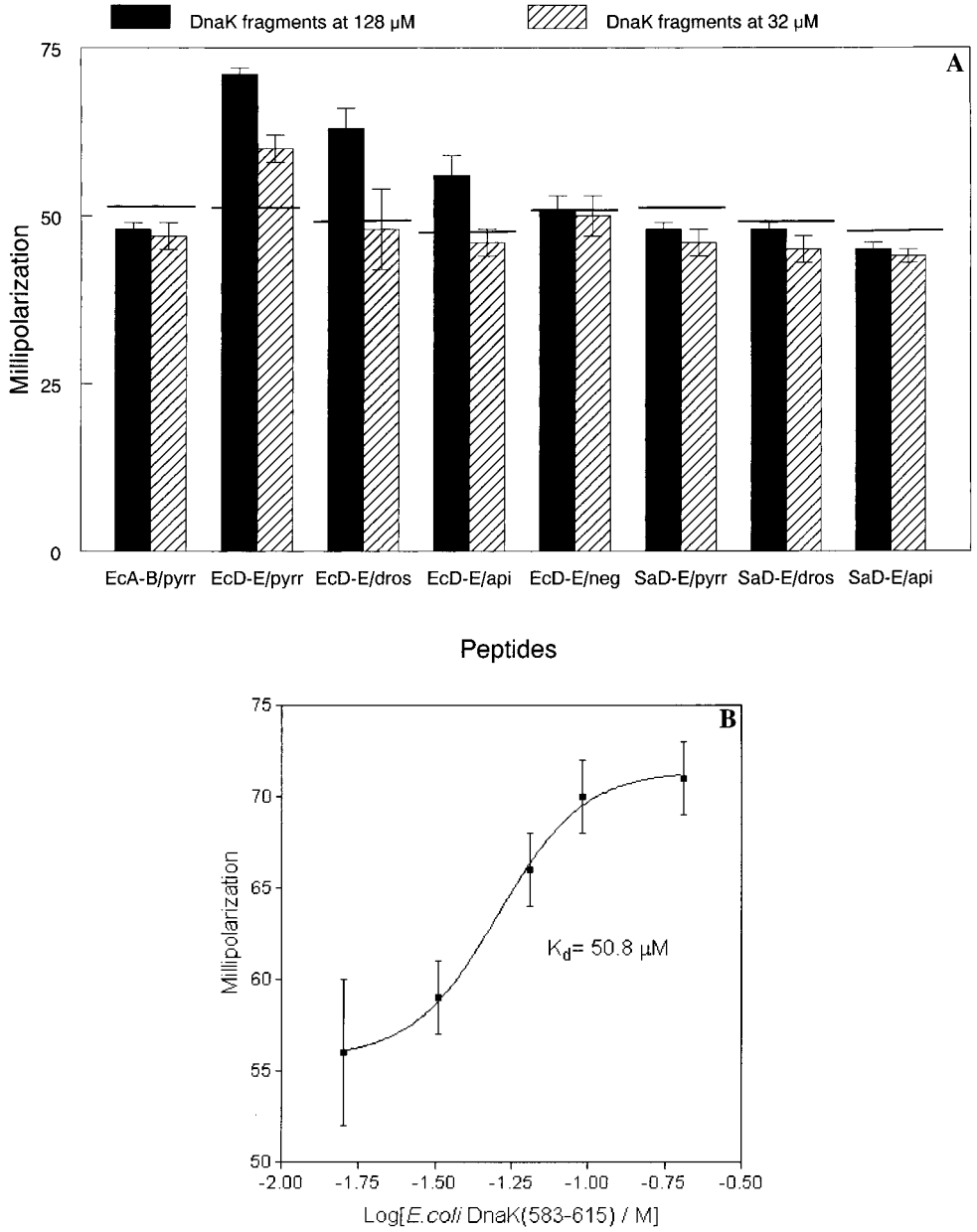

FIGURE 5: Fluorescence polarization analysis of binding of synthetic DnaK fragments to labeled pyrrhocoricin, drosocin, and apidaecin. Panel A shows the assay results against three DnaK fragments, *E. coli* 513−551, referred to as EcA-B, *E. coli* 583−615, referred to as EcD-E, and *S. aureus* 554−585, referred to as SaD-E. The slashes separate the DnaK helix regions and the labeled antibacterial peptides. pyrr stands for pyrrhocoricin, dros stands for drosocin, and api stands for apidaecin. The term neg stands for the negative control fluorescein-labeled peptide NTDGSTDYGILQINSR. The horizontal lines crossing the bars represent the polarization value of the individual labeled peptides at 1 nM concentration, without addition of any DnaK fragment. These background readings were recorded immediately before or after the test peptides were assayed. Panel B shows the dose−response curve of the *E. coli* D−E helix hinge peptide 583−615 against N-terminally fluorescein-labeled pyrrhocoricin. For these measurements 10 consecutive readings were averaged. Both experiments representing the two panels were repeated with freshly lyophilized samples and yielded very similar results.

(Figure 6, panel A). During docking 2, the orientation of pyrrhocoricin stayed antiparallel with helix E, and its N-terminal region stayed in close contact with the hinge and helix D (Figure 6, panel B). The conformation of the N-terminal region of pyrrhocoricin in the bound state resembled that of the isolated peptide, but from residue 14 a turn-like structure was stabilized which moved away the C-terminus of the peptide from helices D and E.

DISCUSSION

Recently, we documented that the proline-rich antibacterial peptide family drosocin−pyrrhocoricin−apidaecin interacts with the LPS of Gram-negative bacteria and the bacterial chaperonine/heat shock proteins GroEL and DnaK (*11*). On the basis of comparison with the amino acid sequences of pyrrhocoricin-responsive and pyrrhocoricin-nonresponsive bacterial strains, we also suggested that the binding to DnaK takes place somewhere between the conventional peptide-binding pocket and the extreme C-terminus, but experimental proof was not provided to support this hypothesis. In addition, direct evidence to support our suggestion that these peptides inhibit chaperone-assisted protein folding was not presented, except that we showed that an inactive pyrrhocoricin analogue does not bind to *E. coli* DnaK (*11*). In the

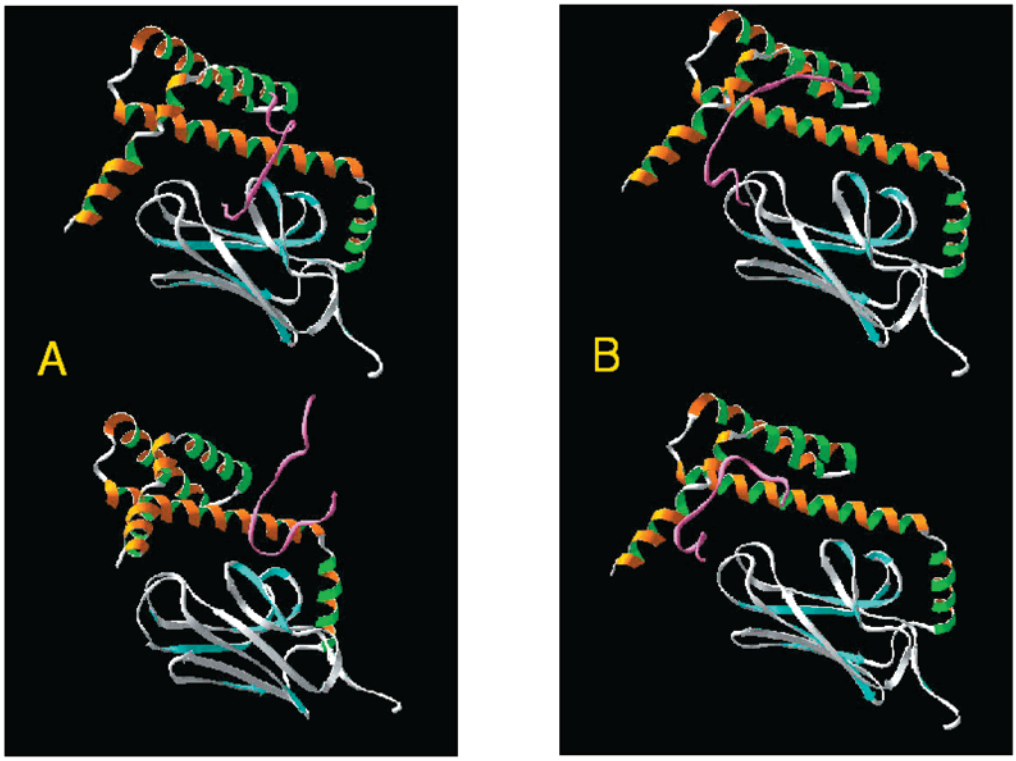

FIGURE 6: Characteristic structures of pyrrhocoricin and the C-terminal region of *E. coli* DnaK as they were generated by the flexible docking process. The details of the calculations are found in the Materials and Methods section. Panel A shows docking 1, as described in the Results section, and panel B shows docking 2. The initial structures are represented by the top models, and the final structures are represented by the bottom models. The blue-white domain corresponds to the peptide-binding cavity, the orange-green domain corresponds to the multihelical lid, and the purple structure corresponds to pyrrhocoricin.

current report we identified the pyrrhocoricin-binding site on *E. coli* DnaK and correlated the antibacterial activity with inhibition of DnaK's two major functions: ATPase activity and protein folding. These experiments clearly demonstrated that the binding site of pyrrhocoricin in *E. coli* DnaK is located in the neighborhood of the hinge between C-terminal helices D and E. As pyrrhocoricin diminished the ATPase activity of recombinant DnaK, the D−E helix region is likely one of those C-terminal domains that allosterically influence the ATPase actions. A weak binding to drosocin was observed with the binding site slightly shifted toward the D helix. Drosocin did not influence the ATPase activity. Nevertheless, both peptides inhibited the DnaK-mediated protein folding as we demonstrated by the significant reduction in β-galactosidase and by the less prominent, but still observable reduction of the alkaline phosphatase activities. Pyrrhocoricin's dual actions compared to drosocin's single effect explains the markedly increased bacterial killing potency of the former peptide (*9*).

Unlabeled pyrrhocoricin kills bacteria in the mid-nanomolar concentration range, but the activity decreases considerably when the N-terminus is labeled with fluorescein or biotin (*12*). Still, the 5 μM IC_{50} of the fluorescein-labeled peptide is below the mid-micromolar binding constant to the DnaK D−E helix hinge fragment as we presented it here. This difference in binding/killing efficacy can be explained on the basis of three different scenarios. First, the antibacterial peptides reach the intracellular milieu by a complex transport mechanism (*10*), which can allow intracellular accumulation of the peptide for effective killing. Second, the antibacterial peptide may bind to full-sized DnaK protein with a considerably higher efficacy than it does to the isolated peptide fragment. If it is indeed true that pyrrhocoricin sees not only the primary sequence but also the secondary structure of the D−E helix hinge region, it should interact with the full-sized protein much more efficiently. Third, the D−E helix region is just one of the pyrrhocoricin-binding sites on DnaK. According to the data presented in this paper, the D−E helix represents the specific binding site of the peptide, but on the basis of our previous report and the nonspecific binding spots on the peptide blot, there are additional pyrrhocoricin-binding sites which could contribute to the efficacious bacterial killing.

The current methods of measuring the protein folding efficiency of the heat shock proteins are far from being perfected. The catalytic potency of a number of enzymes produced by *E. coli* can be evaluated, and we hypothesized that inhibition of the chaperone-assisted protein folding by the proline-rich peptides will result in a decreased level of active enzyme production, and the differences in the enzymatic activity can be detected. We chose alkaline phosphatase and β-galactosidase, two enzymes that are encoded by the *E. coli* TG-1 strain genome and indeed abundantly expressed (*31*, *32*). In fact, *E. coli* DnaK null mutants biosynthesize and secrete a number of enzymes at a significantly reduced level, including alkaline phosphatase and β-galactosidase (*33*). Along with these studies, we wanted to compare the antibacterial activity and enzyme inactivation potency of the peptides, but this was not possible. To be able to reliably measure the enzymatic activity, we had to use bacteria in a colony number well exceeding that required by the standard antibacterial assay (*7*). Although the peptides did not fully kill the larger batch of bacteria even if applied well over their minimal inhibitory concentration values, the changes

in the enzymatic activity could be easily detected. Actually, the increase of enzymatic activity as the examination time progressed from 1 to 6 h could be used as an internal control of the validity of the assay.

Pyrrhocoricin and perhaps drosocin and apidaecin as well appeared to bind to DnaK at the multihelical lid region, located just above the conventional peptide-binding cavity. The function of this multihelical lid is the frequent opening and closing of the "entrance" to the pocket, thereby regulating the protein folding process (*30*). When preparing DnaK fragments that may constitute the binding site for the proline-rich antibacterial peptides, we first concentrated on the connections between the helices that can serve as a driving force for the opening and closing of the pocket. The most probable site is the hinge between helices A and B (*30*) although a latch around residues 536−538, in the middle of helix B, was also proposed to flip from a closed position in the adenosine 5′-diphosphate (ADP) state to an open position in the ATP state (*24*). In our hands, neither of the labeled antibacterial peptides bound to the DnaK 513−551 fragment that contains both of these potential movable domains. Pyrrhocoricin, however, bound to another possible hinge region, at the junction between helices D and E, closer to helix E. Drosocin also weakly bound to the D−E helix hinge fragment, but it approached it from the D helix side.

It is an intriguing question why the antimicrobial peptides produced by *Drosophila melanogaster* and *Pyrrhocoris apterus* kill bacteria by the same mechanism but have slightly different binding sites on bacterial DnaK. It was earlier argued that the sequence differences among the proline-rich antimicrobial peptides reflect the ingenious "combinatorial chemistry" capabilities of insects (*4*), the most abundant class of animals which achieved remarkably low extinction rates during evolution (*34*). Based on this, if the flies or the true bugs had the same main bacterial enemy, the peptides should have taken shape to bind to the same site on *E. coli* DnaK. According to our studies they do not, which indicates that these different families of insects face different life-threatening bacteria. It is possible that the limited number of bacterial strains that we use to test the antibacterial properties of these natural products masks the identity of the real strains these peptides are made against. Alternatively, the peptides expressed by flies and bugs bind on shifted sites on DnaK to avoid a potential cross-reaction with the DnaK sequences of the individual insects themselves. However, this scenario would not explain the lack of drosocin binding to the E helix region of *E. coli* DnaK. A comparison of the amino acid sequences of *D. melanogaster* DnaK 595−612 (ELTRHCSPIMTKMHQQGA) and the corresponding *E. coli* DnaK 589−606 (ELAQVSQKLMEIAQQQHA) reveals major dissimilarities and suggests that a peptide capable of binding to the *E. coli* heat shock protein will not be able to attach to the insect's own DnaK. As far as we know, the sequence of the DnaK protein of *P. apterus* has not been published yet.

The modeling indicated that pyrrhocoricin did not preferably bind to the peptide-binding pocket (docking 1). The apparent conflict with the results of the dot blot and the fluorescence polarization could be resolved by considering that the physical measurements of the interaction did not provide us with the exact site of the binding. Actually, the peptide could have bound to an outer surface of the peptide-binding pocket, which is readily available in the synthetic, only partially folded protein fragment but otherwise not accessible in full DnaK protein. The results of docking 2 is in full agreement with those of the fluorescence polarization measurements that showed that the N-terminal region of pyrrhocoricin (residues 1−9) is the strongest binder to the D−E helix region of DnaK, and the binding surface probably extends further down to residues 11−12. Apparently, the strong binding of pyrrhocoricin to the D−E helix hinge region permanently closes the lid over the peptide binding cavity and prevents chaperone-assisted protein folding.

The success of connecting the antibacterial activity of pyrrhocoricin and drosocin with the mechanism of action as indicated by the β-galactosidase assay allows us to reformulate our thinking of the most suitable assay conditions to gauge the efficacy of the proline-rich peptide family. The validated conditions pharmaceutical companies prefer often fail to reproduce the results obtained at research laboratories. For example, during these validated assay conditions pyrrhocoricin failed to kill even that particular *E. coli* strain (ATCC 25922) that had been used successfully for our in vivo efficacy assay (*12*). In support, a most recent review, dealing with protein targets of antimicrobial compounds, declared that it is now widely accepted that the traditional screening methods, based on direct measurements in living cells of the inhibitory capacities of particular compounds, are unlikely to generate many promising molecules (*3*). This is understandable in light of the assay readout. The validated assay is concerned with the reproduction of bacteria in specific media and conditions most suitable for bacterial growth, conditions not present in vivo in mammals. In support, another recent review on antibacterial peptides noted that a number of factors deactivate otherwise potent antibacterial peptides in vitro (*6*). Therefore, we need to develop assays, the readout of which is more representative for the mode of action of the proline-rich peptides and the in vivo conditions. Actually, our enzyme assays, especially the assay for the presence of β-galactosidase activity, appear to be suitable to assess the antibacterial efficacy of the pyrrhocoricin−drosocin−apidaecin-based peptides.

We noticed that both the alkaline phosphatase and the β-galactosidase activities diminished well before the bacteria died, both in time and in extent. Another idea that comes from the diminished enzymatic activity of the bacteria before they are actually killed is the potential of the proline-rich peptides to augment the activity of other, membrane-disrupting antibacterial peptides, such as cecropin or defensin. These latter peptides destabilize the bacterial membrane for both Gram-negative (cecropin) and Gram-positive (defensin) strains (*4*). If these membrane-active peptides are applied below their active dose (and therefore well below their toxic dose), these peptides could open up the bacterial membrane and allow the proline-rich peptides to enter the cells and bind and inhibit bacterial DnaK faster and at lower concentrations than they would do without the combination therapy.

The characterization of the pyrrhocoricin- and drosocin- and perhaps apidaecin-binding site on *E. coli* DnaK identifies the D−E helix hinge and the region around it as ideal targets for the design of strain-specific antibacterial peptides. This domain is remarkably dissimilar in various bacterial and mammalian DnaK sequences, suggesting that it is possible to design peptides that selectively kill bacteria but are without toxicity to experimental animals or humans. For such a

design process to take place the pyrrhocoricin−*E. coli* DnaK contact residues need to be identified first. This task seems to be relatively straightforward with cocrystallizing the peptide and the protein or its peptide-binding fragment or to use NMR and transferred nuclear Overhauser effects on the same samples. More difficult is to solve the problem by modeling. Presently, the X-ray coordinates of DnaK of *E. coli*, PDB ID 1DKX (*24*), are the only available known structures for heat shock proteins. For other bacterial and fungal heat shock proteins, since they have some (but not always significant) sequence similarity to *E. coli* DnaK, the three-dimensional structures can be generated by homology modeling. These studies can be extended to other species as well. Although our main concern is the development of peptides or peptidomimetics that efficiently kill bacteria, the discoveries presented in this paper pave the road for the development of an entire family of biocides. Since all species heavily rely on functional DnaK, the sequence variations in the multihelical lid in general and at the D−E helix junction in particular will allow the design of peptides and peptidomimetics to control not only bacteria but also parasites, insects, or perhaps rodents as well, just to name a few potential applications.

ACKNOWLEDGMENT

The authors thank Dr. Magdalena Blaszczyk-Thurin for critical reading of the manuscript and Philippe Bulet and Jean-Luc Dimarcq for valuable discussions.

REFERENCES

1. Davies, J. (1996) *Nature 383*, 219−220.
2. Tan, Y.-T., Tillett, D. J., and McKay, I. A. (2000) *Mol. Med. Today 6*, 309−314.
3. Giglione, C., Pierre, M., and Meinnel, T. (2000) *Mol. Microbiol. 36*, 1197−1205.
4. Otvos, L., Jr. (2000) *J. Pept. Sci. 6*, 497−511.
5. Park, C. B., Kim, H. S., and Kim, S. C. (1998) *Biochem. Biophys. Res. Commun. 244*, 253−257.
6. Andreu, D., and Rivas, L. (1998) *Biopolymers 47*, 415−433.
7. Bulet, P., Urge, L., Ohresser, S., Hetru, C., and Otvos, L., Jr. (1996) *Eur. J. Biochem. 238*, 64−69.
8. Casteels, P., and Tempst, P. (1994) *Biochem. Biophys. Res. Commun. 199*, 339−345.
9. Hoffmann, R., Bulet, P., Urge, L., and Otvos, L., Jr. (1999) *Biochim. Biophys. Acta 1426*, 459−467.
10. Castle, M., Nazarian, A., Yi, S.-S., and Tempst, P. (1999) *J. Biol. Chem. 274*, 32555−32564.
11. Otvos, L., Jr., O, I., Rogers, M. E., Consolvo, P. J., Condie, B. A., Lovas, S., Bulet, P., and Blaszczyk-Thurin, M. (2000) *Biochemistry 39*, 14150−14159.
12. Otvos, L., Jr., Bokonyi, K., Varga, I., Otvos, B. I., Hoffmann, R., Ertl, H. C. J., Wade, J. D., McManus, A. M., Craik, D. J., and Bulet, P. (2000) *Protein Sci. 9*, 742−749.
13. Zhou, L.-M., Szendrei, G. I., Fossom, L., Maccecchini, M.-L., Skolnick, P., and Otvos, L., Jr. (1996) *J. Neurochem. 66*, 620−628.
14. Bechinger, B., Zasloff, M., and Opella, S. J. (1993) *Protein Sci. 2*, 2077−2084.
15. Steiner, H., Hultmark, D., Engstrom, A., Bennich, H., and Boman, H. G. (1981) *Nature 292*, 246−248.
16. Hoffmann, R., Dawson, N. F., Wade, J. D., and Otvos, L., Jr. (1997) *J. Pept. Res. 50*, 132−142.
17. Otvos, L., Jr., Pease, A. M., Wade, J. D., and Hoffmann, R. (1998) *Protein Pept. Lett. 5*, 207−213.
18. Fields, G. B., and Noble, R. L. (1990) *Int. J. Pept. Protein Res. 35*, 161−214.
19. Szendrei, G. I., Fabian, H., Mantsch, H. H., Lovas, S., Nyeki, O., Schon, I., and Otvos, L., Jr. (1994) *Eur. J. Biochem. 226*, 917−924.
20. Rieger, C. E., Lee, J., and Turnbull, J. L. (1997) *Anal. Biochem. 246*, 86−95.
21. Lundblad, J. R., Laurance, M., and Goodman, R. H. (1996) *Mol. Endocrinol. 10*, 607−612.
22. van der Spoel, D., van Bunren, A. R., Apol, E., Meulenhoff, P. J., Tielman, D. P., Sijbers, A. L. T. M., Hess, B., Feenstra, K. A., Lindahl, E., van Drunen, R., and Berendsen, H. J. C. (1999) *GROMACS User Manual version 2.0*, Groningen, The Netherlands (http://md.chem.rug.nl/∼gmx).
23. Kabsch, W., and Sander, C. (1983) *Biopolymers 22*, 2577−2637.
24. Zhu, X., Zhao, X., Burkholder, W. F., Gragerov, A., Ogata, C. M., Gottesman, M. E., and Hendrickson, W. A. (1996) *Science 272*, 1606−1614.
25. Berman, H. M., Westbrook, J., Feng, Z., Gilliland, G., Bhat, T. N., Weissig, H., Shindyalov, I. N., and Bourne, P. E. (2000) *Nucleic Acids Res. 28*, 235−242.
26. Liberek, K., Skowyra, D., Zylicz, M., Johnson, C., and Georgopoulos, C. (1991) *J. Biol. Chem. 266*, 14491−14496.
27. Davis, J. E., Voisine, C., and Craig, E. A. (1999) *Proc. Natl. Acad. Sci. U.S.A. 96*, 9269−9276.
28. Freeman, B. C., Myers, M. P., Schumacher, R., and Morimoto, R. I. (1995) *EMBO J. 14*, 2281−2292.
29. Tsai, M.-Y., and Wang, C. (1994) *J. Biol. Chem. 269*, 5958−5962.
30. Mayer, M. P., Schroder, H., Rudiger, S., Paal, K., Laufen, T., and Bukau, B. (2000) *Nat. Struct. Biol. 7*, 586−593.
31. Stec, B., Holtz, K. M., and Kantrowitz, E. R. (2000) *J. Mol. Biol. 299*, 1303−1311.
32. Nielsen, D. A., Chou, J., MacKrell, A. J., Casadaban, M. J., and Steiner, D. F. (1983) *Proc. Natl. Acad. Sci. U.S.A. 80*, 5198−5202.
33. Wolska, K. I., Lobacz, B., Jurkiewicz, D., Bugajska, E., Kuc, M., and Jozwik, A. (2000) *Microbios 101*, 157−168.
34. Labandeira, C. C., and Sepkoski, J. J., Jr. (1993) *Science 261*, 310−315.
35. Liberek, K., Marszalek, J., Ang, D., Georgopoulos, C., and Zylicz, M. (1991) *Proc. Natl. Acad. Sci. U.S.A. 88*, 2874−2878.
36. Giacomenti, A., Cirioni, O., Barchiesi, F., Del Prete, M. S., and Scalise, G. (1999) *Peptides 20*, 1265−1273.

BI002656A